Meso alkynylated tetraphenylethylene (TPE) and 2,3,3-triphenylacrylonitrile (TPAN) substituted BODIPYs

*Bhausaheb Dhokale, Thaksen Jadhav, Shaikh M. Mobin, and Rajneesh Misra**

*E-mail: rajneeshmisra@iiti.ac.in

Department of Chemistry, Indian Institute of Technology Indore,

Indore- 452 017, India.

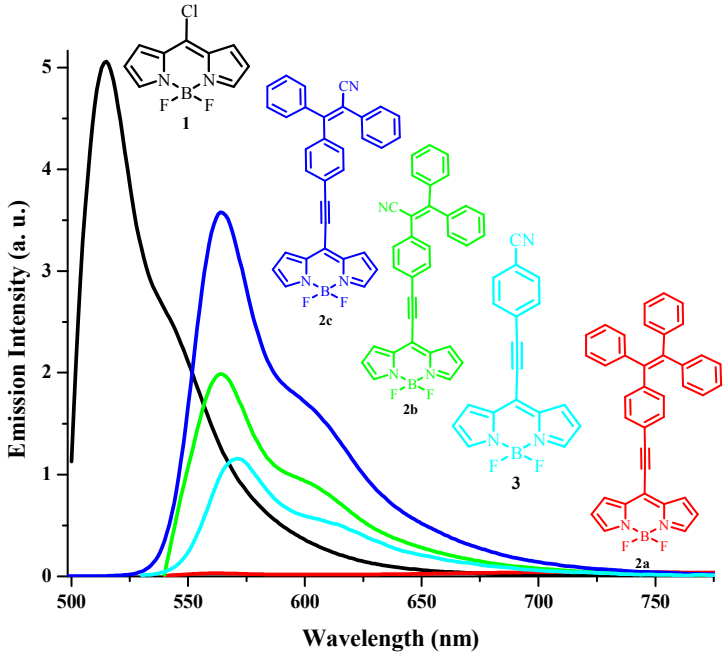

Abstract

The tetraphenylethylene (TPE) substituted BODIPY **2a**, and 2,3,3-triphenylacrylonitrile (TPAN) substituted BODIPYs **2b** and **2c** were designed and synthesized by the Pd-catalyzed Sonogashira cross-coupling reaction. Their photophysical, and electrochemical properties were investigated. The BODIPY **2a** exhibits strong D-A interaction with poor fluorescence quantum yield. The BODIPYs **2b** and **2c** show red shifted absorption and emission with higher

fluorescence quantum yield compared to BODIPY **2a**. The photonic properties of BODIPYs **2a – 2c** were compared with 4-ethynylbenzonitrile substituted BODIPY **3** and phenylacetylene substituted BODIPY **4**. The results reveal that the electron donating group at the *meso* position of BODIPY blue shifts the absorption and emission with decreased fluorescence quantum yield, whereas the electron withdrawing group at the *meso* position of BODIPY red shifts the absorption and emission with enhanced quantum yields. The single crystal structures of BODIPYs **2a** and **2b** reflect the planar orientation of *meso* substituent and the BODIPY core, which leads to close π-π stacking. The extensive π-π stacking and strong donor–acceptor (D-A) interaction makes these BODIPYs AIE inactive. The experimental observations were supported by DFT calculation.

Introduction

The BODIPY fluorophores are known for their strong absorption and emission with excellent fluorescence quantum yield.[1] Their unique photonic properties make them attractive candidate for wide range of applications.[2] The spectral properties of the BODIPY fluorophore can be tuned by introducing different functionalities at α, β and *meso* positions.[3] The BODIPYs are strong acceptor owing to their electron deficient nature.[4] Recently we have shown that the electron deficiency of 8-chloro BODIPY is sufficient to oxidize aliphatic *tert*-amines.[5] A variety of donor groups were introduced at the *meso* position of the BODIPY through alkyne linkage, which resulted in strong donor-acceptor (D-A) systems. Introduction of alkyne linkage at the *meso* position induces planarity between the *meso* substituent and the BODIPY, which improves the electronic communication.[6] The donor group at the *meso* position of the BODIPY leads to blue shifted absorption with poor quantum yield.[7] To the best of our knowledge the effect of

acceptor group on the photonic properties of *meso* alkynylated BODIPYs has not been explored yet.

The conventional fluorophores suffer from aggregation caused quenching (ACQ), which quenching of fluorescent in solid state. This problem was overcome by introducing the concept AIE.[8] The AIE active molecules are poorly emissive in solutions at the same time highly emissive in solid state. Tetraphenylethylene (TPE) and 2,3,3-triphenylacrylonitrile (TPAN) are propeller shaped molecules, known for their unique ability to promote aggregation induced emission (AIE) in different fluorophores.[9] The electronegative groups like (-CN, -F) are known to induce the aggregation induced enhanced emission (AIEE).[10] We have chosen the TPE and TPAN functionalities and coupled them with the BODIPY through alkyne linkage at the *meso* position to study their effect on the photonic properties of BODIPYs.

Herein, we report the design and synthesis of *meso* alkynylated TPE substituted BODIPY **2a**, and TPAN substituted BODIPYs **2b**, and **2c** by Sonogashira cross-coupling reaction. Their photonic properties were studied and compared with 4-ethynylbenzonitrile substituted BODIPYs **3** and phenylacetylene substituted BODIPYs **4** (Chart 1). The planar orientation of *meso* substituent and the BODIPY ensures the strong electronic communication between them. The photonic properties were strongly influenced by the nature of substituents and the π-π stacking interaction.

Results and Discussion

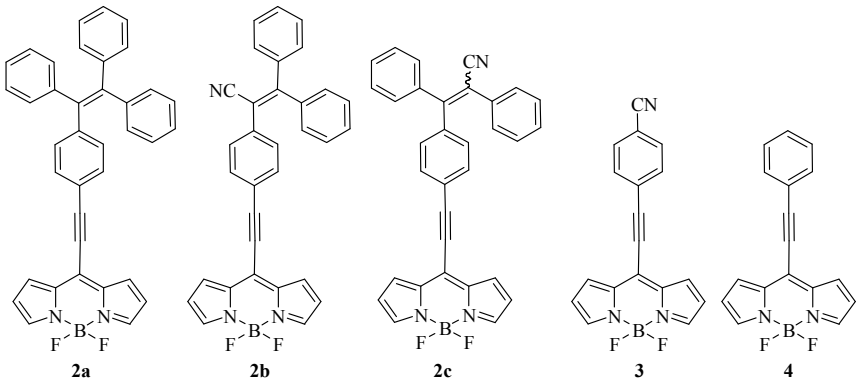

Chart 1. The TPE substituted BODIPY **2a**, TPAN substituted BODIPYs **2b**, **2c** and BODIPYs **3** and **4**.

The TPE substituted BODIPY **2a**, TPAN substituted BODIPYs **2b**, **2c**, BODIPYs **3** and **4** were synthesized by the Pd-catalyzed Sonogashira cross-coupling reaction of 8-chloro BODIPY **1** with the respective alkynes (Scheme 1). The precursor 8-chloro BODIPY **1** was synthesized by the reaction of dipyrrylketone with $POCl_3$ followed by *in situ* deprotonation by the base triethylamine and complexation with BF_3.etherate. [11]

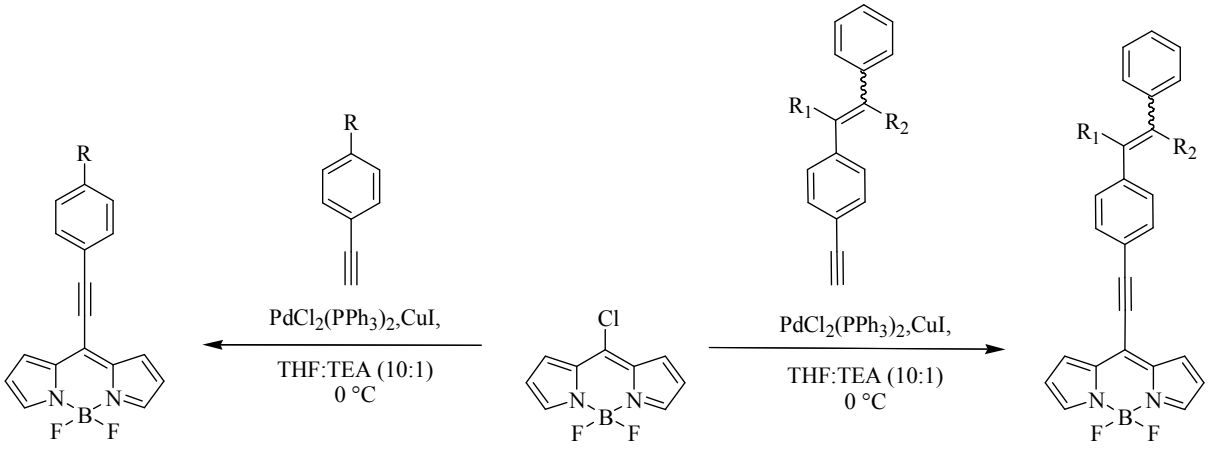

3 - 4 **1** **2a - 2c**

R	BODIPY
CN	**3**
H	**4**

Alkyne	R_1	R_2	BODIPY
a	Ph	Ph	**2a**
b	CN	Ph	**2b**
c	Ph	CN	**2c**

Scheme 1. Synthesis of TPE substituted BODIPY **2a**, TPAN substituted BODIPYs **2b**, **2c** and BODIPYs **3** and **4**.

The TPE-alkyne **a** was synthesized using reported procedure from bromo-TPE (Scheme S1, ESI).[12] The TPAN-alkyne **b** was synthesized by the Sonogashira cross-coupling reaction of bromo-TPAN with TMS-acetylene, followed by deprotection of TMS group by K_2CO_3 in overall 69 % yield (Scheme 2).[13] The TPAN-alkyne **c** was synthesized by the condensation reaction of 4-bromo benzophenone with benzyl nitrile in the presence of base NaH, followed by the Sonogashira cross-coupling reaction with TMS-acetylene and deprotection of TMS group by K_2CO_3 in overall 29 % yield (Scheme 3).

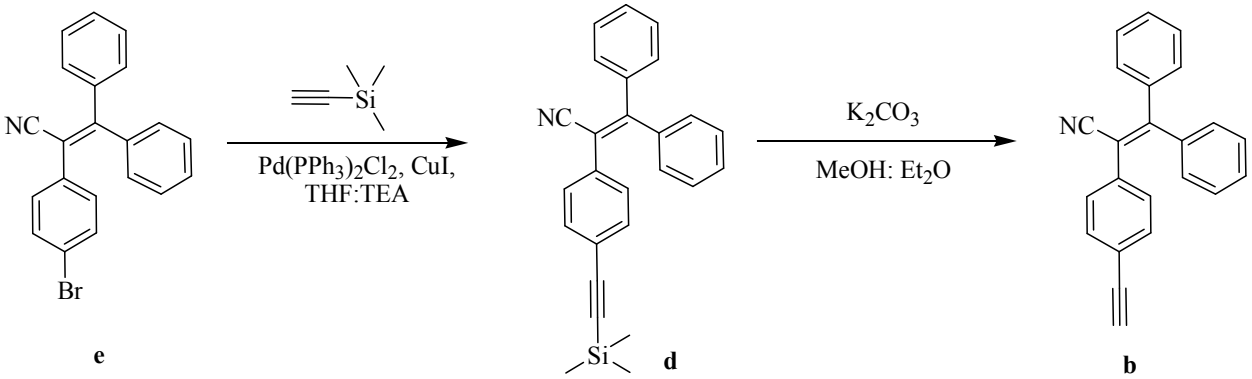

Scheme 2. Synthesis of 2-(4-ethynyl-phenyl)-3,3-diphenylacrylonitrile (TPAN-alkyne **b**).

The Sonogashira cross-coupling reaction of 8-chloro BODIPY **1** with alkynes **a**, **b** and **c** at 0 °C resulted TPE substituted BODIPY **2a**, and TPAN substituted BODIPYs **2b**, and **2c** in 70 %, 74 % and 72 % yields respectively (Scheme1). The TPAN substituted BODIPY **2c** is mixture of *cis* and *trans* isomers. Its purification by repeated column chromatography and recrystallization was unsuccessful (Figure S1; ESI), and reported as 1:1 mixture. The BODIPYs **3** and **4** were synthesized by the Sonogashira cross-coupling reaction of 8-chloro BODIPY **1** with 4-ethynylbenzonitrile and phenylacetylene in 52 % and 76 % yields respectively (Scheme 1).

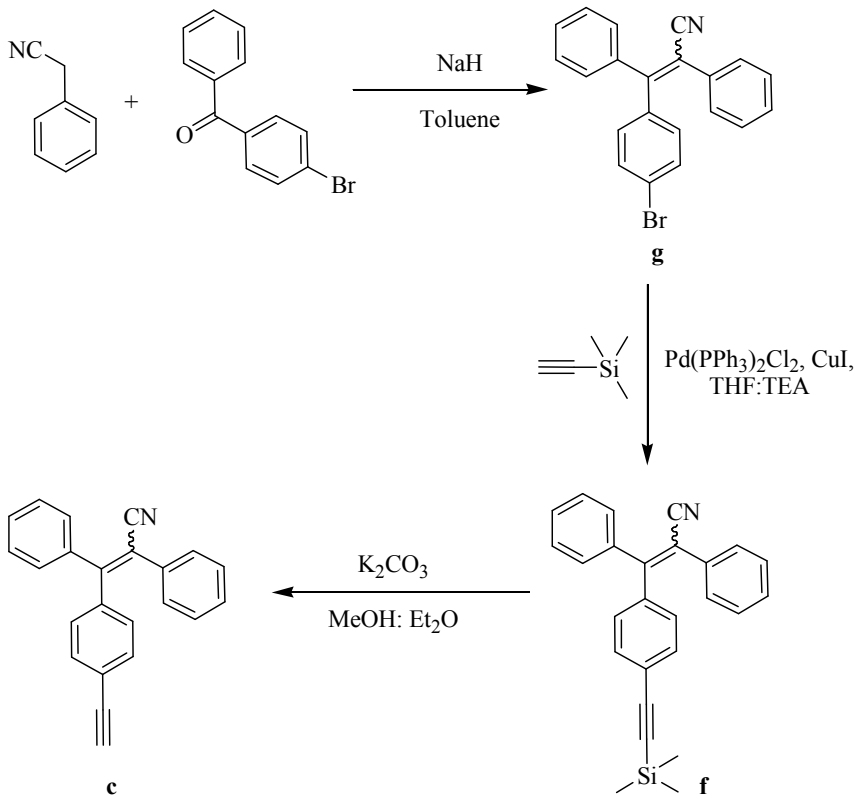

Scheme 3. Synthesis of 2,3-diphenyl-3-(4-ethynylphenyl)-acrylonitrile (TPAN-alkyne **c**).

The BODIPYs were well characterized by ^{1}H NMR, ^{13}C NMR, ^{11}B NMR and HRMS techniques. The BODIPYs **2a**, and **2b** were also characterized by single crystal X-ray crystallography.

The ^{1}H NMR spectra of BODIPYs **2a – 2c**, **3** and **4** shows the *α, β* and *β′* protons, at ~ 7.8, 6.5 and 7.3 δ ppm respectively. The *meso* phenyl protons of BODIPY, **3** and **4** behave in unusual manner. In BODIPY **4** the five phenyl protons appear as multiplets in two sets at δ = 7.65 and δ = 7.45, whereas in BODIPY **3** the four phenyl protons appear as singlet at δ = 7.75 (Figure S2; ESI). This indicates that the cyano group in BODIPY **3** minimizes the dipole moment (μ = 1.24) compared to BODIPY **4** (μ = 6.82) making the four phenyl protons equivalent.

Photophysical Properties

The electronic absorption spectra of BODIPYs **1**, **2a – 2c** and **3** were recorded in THF (Figure 1), and the corresponding data are shown in Table 1. The TPE substituted BODIPY **2a** absorbs at 543 nm and the TPAN substituted BODIPYs **2b**, and **2c** absorb at 546 nm. Compared to the 8-chloro BODIPY **1**, the BODIPY **2a** exhibits red shift of 41 nm, whereas the BODIPYs **2b** and **2c** exhibit red shift of 44 nm. The red shift in the absorption is attributed to the extension of π-conjugation. The higher red shift of the TPAN substituted BODIPYs **2b** and **2c**, than TPE substituted BODIPY **2a** is attributed to the stabilization of LUMO due to the acceptor group (-CN) at the *meso* position.[14] The effect of (-CN) acceptor cyano on the red shift in absorption is also evidenced from the absorption of BODIPY **3** at 552 nm, which is highly red shifted than BODIPY**4** and BODIPYs **2a** – **2c**. The BODIPYs (**2a**, **2b**, **2c**, **3** and **4**) exhibit negative solvatochromism with increasing solvent polarity (Figure S3-S7; ESI).

The TD-DFT calculation was performed on TPAN substituted BODIPY **2b** to understand the origin of absorption bands. The TD-DFT calculation was performed by using two different methods B3LYP and CAM B3LYP at 6-31G(d) level in THF solvent using the IEFPCM formulation for solvent effects. The calculation performed by B3LYP method show more close resemblance with the experimental data (Figure S17). The oscillator strengths and configurations of vertical transitions are shown in Table S4 and the molecular orbitals involved in the transitions are displayed in Figure S18 (ESI). The TD DFT calculations reveals that the main absorption band at ~585 nm is contributed by the transitions from HOMO, HOMO-1 and HOMO-2 to LUMO, whereas the band at ~380 nm is contributed by the transitions from HOMO-2 and HOMO-3 to LUMO; and from HOMO and HOMO-1 to LUMO+1.

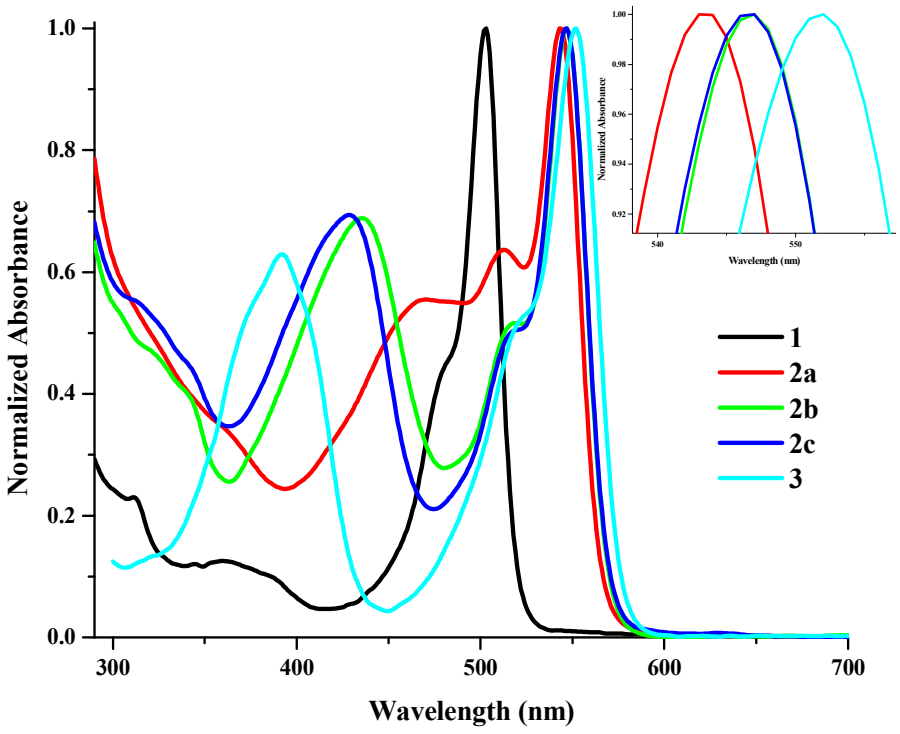

Figure 1. Normalized electronic absorption spectra of BODIPYs **1**, **2a – 2c** and **3** in THF.

The emission studies of BODIPYs **1**, **2a – 2c** and **3** were performed in THF (Figure 2); and the corresponding data are shown in Table 1. The red shift in the emission spectra follows the order **3**>**2c**=**2b**>**2a**>**4**>**1**. The TPE substituted BODIPY **2a** exhibits dual emission from locally excited (LE) state at 561 nm, and from charge transfer state at 731 nm with poor quantum yield (ϕ_F = 0.02), whereas the TPAN substituted BODIPYs **2b** and **2c** emit only from the LE state at 564 nm with higher fluorescence quantum yield (ϕ_F = 0.41 and 0.43 respectively).

The BODIPY **3** exhibits red shifted emission at 571 nm, whereas the BODIPY **4** emits at 556 nm. The cyano group in BODIPY **3**, red shifts the absorption and emission, but decreases the fluorescence quantum yield Compared to BODIPY **4**. The fluorescence quantum yield of BODIPYs **1 – 4** follows the order **1**>**4**>**2c**>**2b**>**3**>**2a**.

The TPE substituted BODIPY **2a** and TPAN substituted BODIPYs **2b** and **2c** are AIE inactive. This suggests that fluorescence of TPE substituted BODIPY **2a** in solution is quenched

due to the charge transfer from donor TPE to the acceptor BODIPY moiety,[15] whereas in TPAN substituted BODIPYs **2b** and **2c** the charge transfer is minimized, which leads to the increased fluorescence quantum yield.

Table 1. Photophysical properties of BODIPYs **1**, **2a – 2c, 3** and **4** in THF.

BODIPY	λ_{max} (nm)	$\varepsilon/10^4$ ($M^{-1}.cm^{-1}$) [a]	λ_{em} [b] (nm)	Stokes shift (cm^{-1})	ϕ_F [c]	HOMO-LUMO gap (eV) (Theoretical)[d]
1	503	10.2	515	463	0.72	-
2a	468		561	4676	0.019	2.63
	543	2.7	731			
2b	435		564	585	0.409	2.72
	546	3.0				
2c	428		564	585	0.428	2.71 (*cis*)
	546	3.1				2.70 (*trans*)
3	552	4.4	571	601	0.440	2.66
4[16]	543	4.3	556	431	0.632	2.78

[a]Recorded at $\lambda_{max,}$ [b]Excited at $\lambda_{max,}$ [c]Determined by using Rhodamine B as standard (ϕ = 0.50, in ethanol), [d]From DFT calculation.

In order to evaluate the effect of cyano (-CN) acceptor at the *meso* position of BODIPY, the quantum yield of BODIPYs **3** and **4** were compared. The cyano group in BODIPY **3** decreases the fluorescence quantum yield compared to the BODIPY **4**. This indicates that the acceptor at the *meso* position of BODIPY increases the quantum yield only upto certain limit **2a>2b>2a** as it minimizes the charge-transfer interaction. However after certain limit the acceptor at the *meso* position quenches the fluorescence, which may be through the oxidative charge transfer from BODIPY, leading to poor quantum yield of BODIPY **3** than **4**.[17] This is in accordance with the work by Nagano et al.[18] Similar trend in photophysical properties was observed in different solvents (Figure S3-S7 and Table S1).

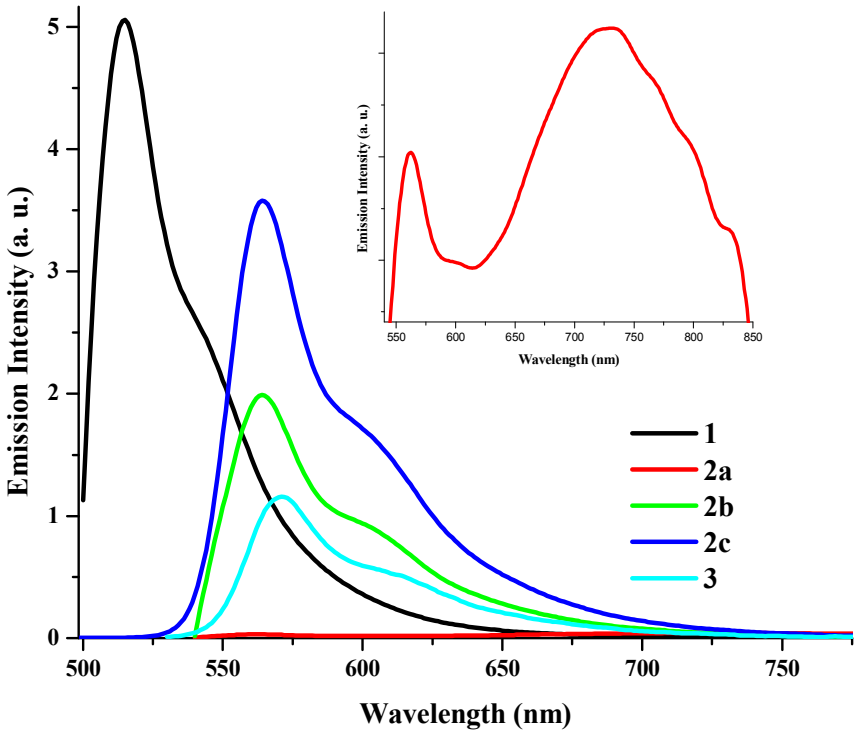

Figure 2. Emission spectra of BODIPYs **1**, **2a – 2c** and **3** (inset shows enlarged view of emission spectra of BODIPY **2a**) in THF.

The TPE substituted fluorophores are poorly emissive in solutions due to the molecular rotations of phenyl rings, and exhibit higher fluorescence quantum yield in aggregate state due to restricted molecular rotation. The AIE properties of TPE substituted BODIPY **2a**, and TPAN substituted BODIPYs **2b** and **2c** were studied by fluorescence spectroscopy in THF-water mixture with varying amount of water fraction. The BODIPYs **2a – 2c** are readily soluble in tetrahydrofuran (THF) and insoluble in water, by increasing the water fraction in the THF-water mixture, the dissolved solute molecules transform into the aggregated particles. The study reveals that the BODIPYs **2a – 2c** are AIE inactive, and show aggregation caused fluorescence quenching (ACQ) (Figure S8-S9; ESI). The fluorescence intensity of BODIPYs **2a – 2c** in pure THF solution decreases with increasing water fraction. Thus the alkynylated TPE and TPAN moieties are unable to induce AIE in BODIPYs like the previously reported TPE substituted BODIPYs.[19] The alkyne linkage increases the distance between TPE and BODIPY, which gives

sufficient space for planarization and π-π stacking. This favors the aggregation caused fluorescence quenching and makes these BODIPYs AIE inactive. The previously reported TPE substituted BODIPYs were AIE active as there was no scope for π-π stacking interactions and aggregation caused fluorescence quenching.

Electrochemical Properties

Table 2. The electrochemical properties of BODIPYs **2a – 2c**, **3** and **4**.

BODIPY	E^3 Oxid[b]	E^2 Oxid[b]	E^1 Oxid[b]	E^1 Red[b]	E^2 Red[b]	E^3 Red[b]
2a	1.81	1.16	0.97	-0.96	-1.25	-1.36
2b	-	1.36	1.11	-0.96	-1.27	-1.39
2c	-	1.45	1.17	-0.90	-1.20	-1.31
3	-	1.27	1.18	-0.90	-1.22	-1.36
4	-	1.33	1.18	-0.99	-1.28	-1.40

[a]The electrochemical analysis was performed in a 0.1 M solution of Bu_4NPF_6 in dichloromethane at 100mV s^{-1} scan rate, versus Fc/Fc^+. [b]Irreversible wave.

The electrochemical properties of the BODIPYs **2a – 2c**, **3** and **4** were investigated by cyclic and differential pulse voltammetric (CV and DPV) techniques (Figure 3 and S10 – S13) and the corresponding data are displayed in Table 2. The First reduction potential of TPE substituted BODIPY **2a**, TPAN substituted BODIPYs **2b**, **2c** and BODIPYs **3** and **4** follows the order **4~2a~2b>2c~3**, which indicates that, compared to BODIPYs **2a** and **4**, the of cyano group in **2b** does not perturbs the LUMO energy level (similar reduction potential) but in **2c** and **3** it stabilizes the LUMO energy level significantly (easier reduction). The first oxidation potential values follow the order **4~3~2c>2b>2a**, which indicates that the *meso* substituents has negligible effect on the HOMO energy level in BODIPYs **2b**, **2c**, **3** and **4** but in BODIPY **2a** the *meso* substituted alkynylated TPE unit destabilizes the HOMO slightly.

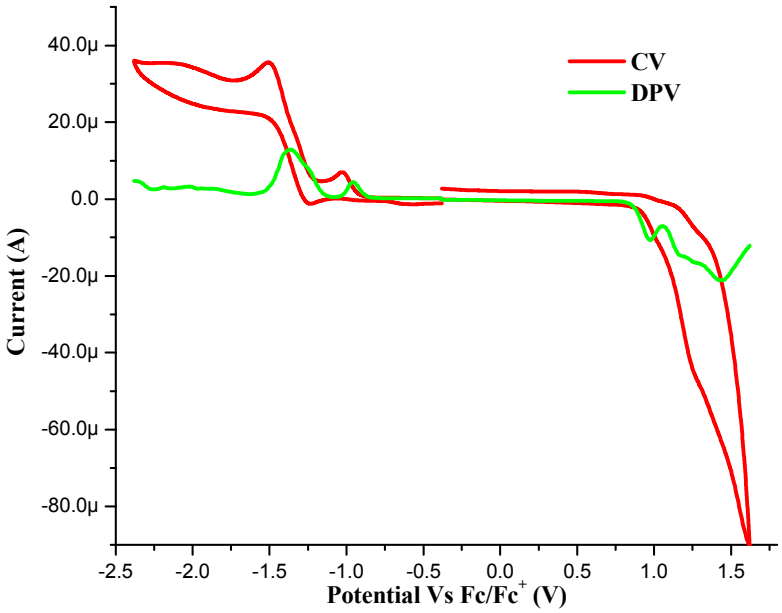

Figure 3. Overlaid CV and DPV plots of TPE substituted BODIPY **2a** in 0.1 M $TBAF_6$ solution in dichloromethane.

DFT Calculation

The Density functional theory (DFT) calculation was performed to understand the electronic structure of the BODIPYs **2 – 4** at B3LYP/6-31G** level. The comparison of geometry optimized structure and crystal structure is shown in Figure S14 (ESI). The crystal structure closely resembles with the energy optimized structure. The energy optimized structures show highly symmetrical BODIPY framework, whereas in crystal structures two pyrrolic rings of BODIPY framework show slight variations in the bond lengths due to the close solid state packing.

The frontier molecular orbital (FMO) plots of BODIPYs **2a – 2c**, **3** and **4** are displayed in Figure 4. The frontier molecular orbital plots of BODIPY **2a** reveals that the HOMO is localized on the TPE moiety, whereas the LUMO is localized on BODIPY moiety. This supports strong D-A interaction and charge transfer from TPE to BODIPY unit. In case of BODIPYs **2b**, **2c**, **3** and

4 the HOMO is localized on the BODIPY moiety and the LUMO is distributed over the entire molecule.

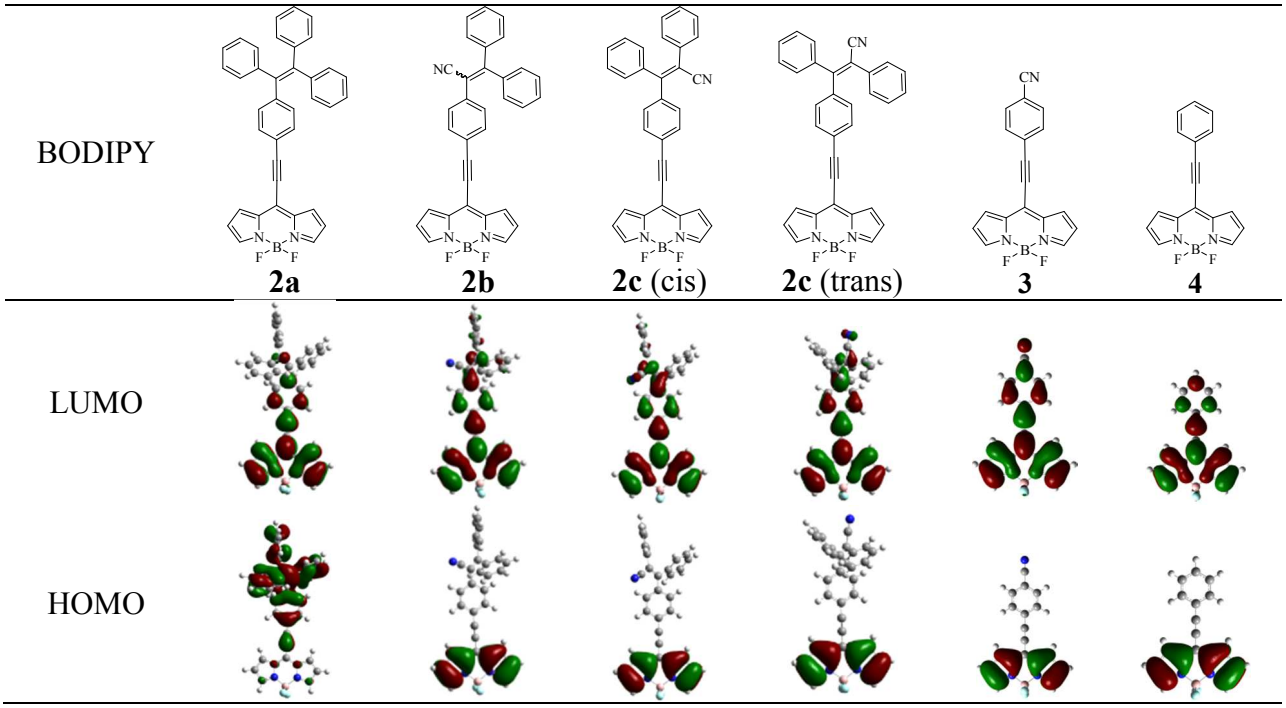

Figure 4. Frontier molecular orbital plots of the BODIPYs **2a**, **2b**, **2c** (*cis*),**2c** (*trans*), **3** and **4** estimated by DFT calculation at B3LYP/6-31G** level.

Crystal Structure

The crystals of BODIPYs **2a** and **2b** for x-ray analysis were grown by slow evaporation of their dichloromethane:hexane solution. The BODIPYs **2a** and **2b** crystalize in triclinic *P*-1 space group (Figure 5). The crystal structure, and data refinement parameters are given in Table S2. The crystal structures of TPE substituted BODIPY **2a**, and TPAN substituted BODIPY **2b** reflect planar BODIPY framework with fluorine atoms projecting above and below the average plane. The distances, and angles of intermolecular interactions are shown in Table S3 (ESI).

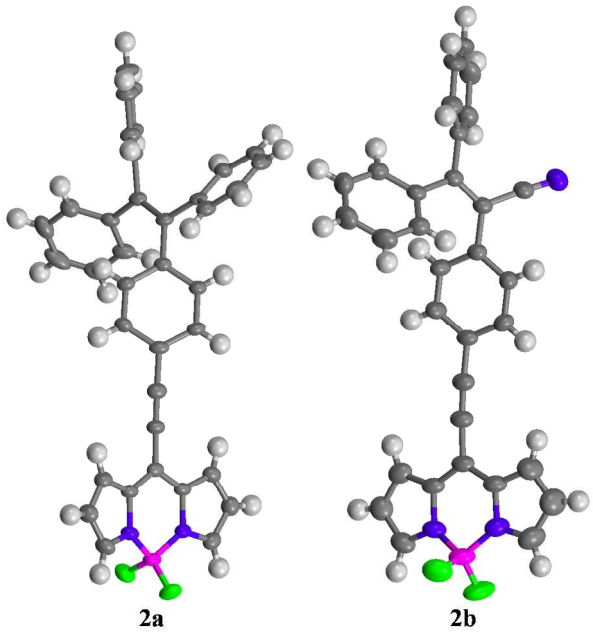

Figure 5. Single crystal structures of TPE substituted BODIPY **2a** and TPAN substituted BODIPY **2b**.

Crystal structure packing

The single crystal structure reveals, extensive hydrogen bonding and close π-π stacking interactions (Figure 6 and 7). In the crystal packing of TPE substituted BODIPY **2a**, the two hydrogen bonding interactions C(13)-H(13)---F(1) and C(17)-H(17)---F(2) and C-H---π interactions C(33)-H(33)---π C(21) (TPE Phenyl) and C(16)-H(16)---π C(34) (TPE Phenyl) and the extensive π-π stacking interaction between BODIPY moieties form a staircase shaped 2D framework. This further leads to complex 3D structural arrangement through C-H---π interactions C(7)-H(7)---π C(34, 35) (TPE Phenyl) and C(36)-H(36)---π C(17) (Phenyl centroid) (Figure 6).

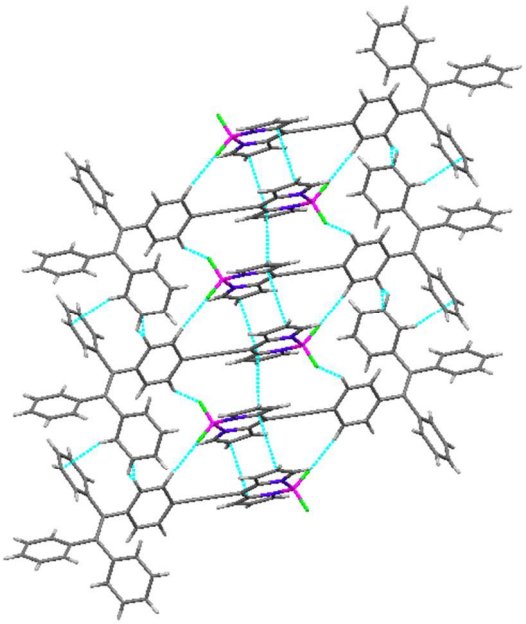

Figure 6. Crystal packing of TPE substituted BODIPY **2a** showing hydrogen bonded π-π stacked staircase shaped 2D network.

The crystal structure packing of TPAN substituted BODIPY **2b** reveals that, the hydrogen bonding interaction B(1)-F(1)---π C(19)(Cyano) and π-π stacking between phenyl ring and the BODIPY central core forms a dimeric framework. These dimers connect to one another via two mutual C(7)-H(7)---F(2) interactions and π-π stacking interaction between two pyrrolic rings to form a sheet. Such sheets are connected to one another via C(24)-H(24)---F(2) and C(26)-H(26)---π C(8) (Pyrrolic centroid) and C(2)-H(2)---F(2) interactions leading to 3D framework. The 3D framework is also stabilized by interaction C(17)-H(17)---π C(24) (TPE Phenyl) (Figure 7).

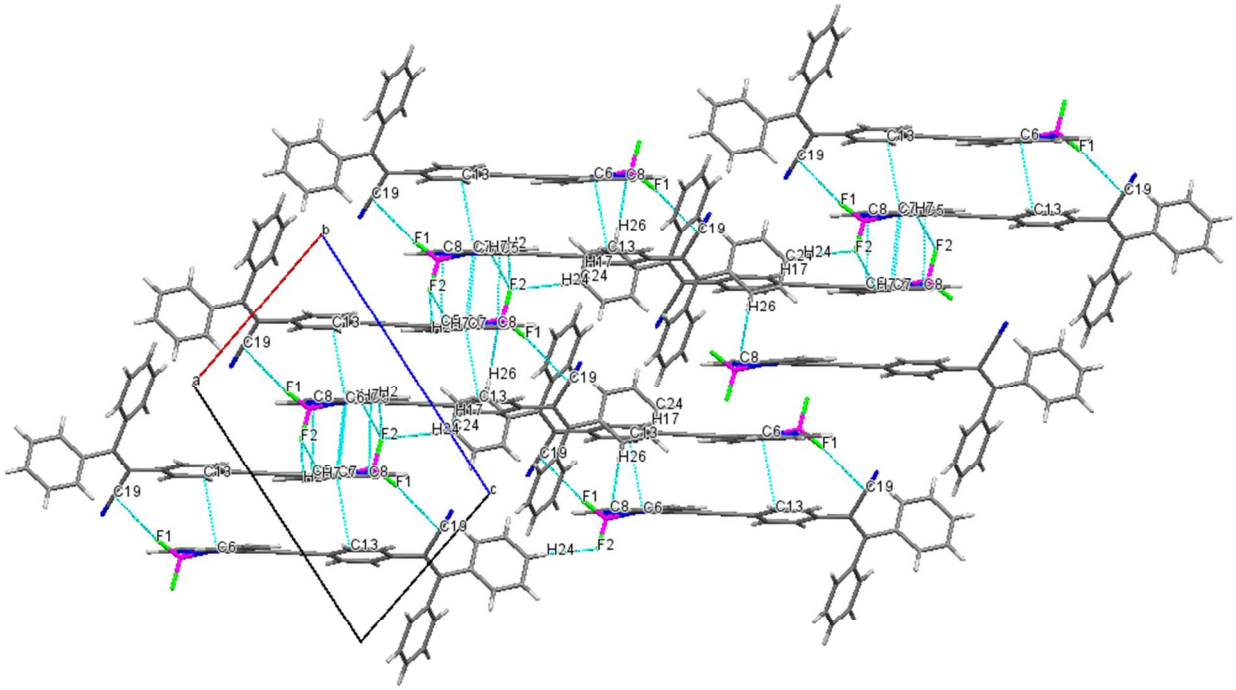

Figure 7. Crystal packing of TPAN substituted BODIPY **2b** showing hydrogen bonded π-π stacked 2D framework.

Conclusions

In summary, The tetraphenylethylene (TPE) substituted BODIPY **2a**, and 2,3,3-triphenylacrylonitrile (TPAN) substituted BODIPYs **2b**, **2c** and 4-ethynylbenzonitrile substituted BODIPYs **3** and phenylacetylene substituted BODIPYs **4** were designed and synthesized by Pd-catalyzed Sonogashira cross-coupling reaction. The planarization induced extensive π-π stacking and strong D-A interaction makes these BODIPY AIE inactive. The introduction of donor group at the *meso* position of BODIPY induces the blue shift in absorption and emission spectra, whereas the electron withdrawing group induces the red shift. The fluorescence quantum yields of TPAN substituted BODIPYs **2b** and **2c** are higher than the TPE substituted BODIPY **2a**, which indicates that, the introduction of cyano group minimizes the CT interaction and increases the fluorescence quantum yield. But this is not true in case of 4-ethynylbenzonitrile substituted

BODIPYs **3** and phenylacetylene substituted BODIPYs **4**, where the introduction of cyano group decreases the fluorescence quantum yields, may be due to the oxidative charge transfer from BODIPY moiety. The detailed photonic applications of these molecules are ongoing in our laboratory.

EXPERIMENTAL SECTION

General methods. Chemicals were used as received unless otherwise indicated. All oxygen or moisture sensitive reactions were performed under nitrogen/argon atmosphere using standard schlenk method. Triethylamine (TEA) was received from commercial source and distilled on KOH prior to use. ^{1}H NMR (400 MHz), ^{13}C NMR (100MHz), ^{11}B NMR (128.37MHz), and ^{19}F NMR (376.49MHz) spectra were recorded on 400 MHz instrument by using $CDCl_3$ as solvent. ^{1}H NMR chemical shifts are reported in parts per million (ppm) relative to the solvent residual peak ($CDCl_3$, 7.26 ppm). Multiplicities are given as: s (singlet), d (doublet), t (triplet), q (quartet), dd (doublet of doublets), m (multiplets), and the coupling constants, *J*, are given in Hz. ^{13}C NMR chemical shifts are reported relative to the solvent residual peak ($CDCl_3$, 77.36 ppm). HRMS were recorded on mass spectrometer. UV-visible absorption spectra of all compounds were recorded on a UV/Vis Spectrophotometer. Fluorescence spectra of all the compounds were recorded on emission spectrophotometer. The voltammograms were recorded in dichloromethane solvent and 0.1 M $TBAF_6$ as supporting electrolyte. The electrodes used were glassy carbon as working electrode, Pt wire as counter electrode and the saturated calomel electrode as reference electrode. The potentials were referenced against Fc/Fc^{+} as per IUPAC guidelines.[20]

Generalized synthetic procedure for the BODIPYs 2a, 2b, 3a and 3b

8-chloro BODIPY **1** (100 mg, 0.44 mmol), and corresponding TPE alkynes (**a**/**b**/**c**) (0.66 mmol) were dissolved in THF:triethylamine (10:1,v/v; 15 ml), and the mixture was cooled to 0 °C using an ice bath. The reaction mixture was purged with argon, and $Pd(PPh_3)_2Cl_2$ (15 mg, 5

mol %), and CuI (8.3 mg, 10 mol %) were added, followed by stirring at 0 – 10 °C for 2 hrs. After complete conversion of starting aryl alkyne **a/b**, the reaction mixture was evaporated to dryness, and the crude product was dissolved in CH_2Cl_2, chromatographed on ~ 70 cm long silica bed using dichloromethane as eluent to get **2** and **3**. The isolated products from column were recrystallized from chloroform: hexane (1:3) mixture as crystalline solid.

Characterization Data

TPE substituted BODIPY 2a: Red crystalline solid. Yield: 70% (170 mg); mp 193 – 194 °C. ^{1}H NMR ($CDCl_3$, 400 MHz, ppm): δ 7.81 (s, 2H), 7.41-7.39 (m, 2H), 7.36 (d, J = 4 Hz; 2H), 7.17-7.10 (m, 11H), 7.07-7.02 (m, 6H), 7.52 (d, J = 4 Hz; 2H); ^{13}C NMR ($CDCl_3$, 100 MHz, ppm): 147.4, 143.5, 143.2, 143.0, 139.8, 136.6, 132.3, 132.0, 131.5, 131.4, 129.0, 128.12, 128.07, 127.9, 127.6, 127.2, 127.0, 118.8, 118.4, 106.7, 84.8; ^{11}B NMR ($CDCl_3$, 128 MHz, ppm) 0.19 (t, $J_{B\text{-}F}$ = 28.16 Hz); HRMS (ESI-TOF) m/z = calculated for $C_{37}H_{25}BF_2N_2$ = 569. 1977 $[M+Na]^+$, measured 569.1961 $[M+Na]^+$; UV/vis (THF) λ_{max} (ε [M^{-1} cm^{-1}]) 543 (2.7×10^4).

TPAN substituted BODIPY 2b: Red crystalline solid. Yield: 74% (243 mg); mp 209 – 210 °C. ^{1}H NMR ($CDCl_3$, 400 MHz, ppm): δ 7.83 (s, 2H), 7.52-7.45 (m, 7H), 7.37-7.31 (m, 5H), 7.27-7.23 (m, 2H), 7.05-7.02 (m, 2H), 6.55 (d, J = 4 Hz; 2H); ^{13}C NMR ($CDCl_3$, 100 MHz, ppm): 159.8, 144.0, 140.1, 138.8, 137.8, 136.7, 132.8, 130.9, 130.6, 130.3, 130.1, 129.7, 129.3, 128.7, 127.0, 120.8, 119.7, 118.6 (b), 110.4, 104.8, 85.2; ^{11}B NMR ($CDCl_3$, 128 MHz, ppm) 0.14 (t, $J_{B\text{-}F}$ = 29.4 Hz); HRMS (ESI-TOF) m/z = calculated for $C_{32}H_{20}BF_2N_3$ = 518.1616 $[M+Na]^+$, measured 518.1617 $[M+Na]^+$; UV/vis (THF) λ_{max} (ε [M^{-1} cm^{-1}]) 546 (3.0×10^4).

TPAN substituted BODIPY 2c: Red crystalline solid. Yield: 72 % (236 mg); mp 206 – 208. ^{1}H NMR ($CDCl_3$, 400 MHz, ppm): 20 H δ 7.85 (d, 2H, J = 8Hz), 7.72 (d, 1H, J = 8Hz), 7.56 (d, 1H, J = 8Hz), 7.49-7.46 (m, 3H), 7.41-7.34 (m, 2H), 7.30-7.21 (m, 7H), 7.12 (d, 1H, J = 8Hz), 7.02

(d, 1H, J = 8Hz), 6.58-6.55 (m, 2H); ^{13}C NMR ($CDCl_3$, 100 MHz, ppm): 156.21, 156.16, 144.1, 142.9, 141.9, 139.7, 138.4, 136.7, 136.6, 134.4, 134.3, 132.8, 132.6, 131.4, 130.8, 130.5, 130.4, 130.0, 129.83, 129.76, 129.5, 129.3, 129.2, 129.03, 128.9, 128.8, 128.7, 128.6, 126.87, 126.76, 122.3, 121.4, 119.80, 119.77, 118.6, 113.1, 113.0, 104.6, 104.5, 85.4, 85.3; ^{11}B NMR ($CDCl_3$, 128 MHz, ppm) 0.19 (t, $J_{B\text{-}F}$ = 28.16 Hz); HRMS (ESI-TOF) m/z = calculated for $C_{32}H_{20}BF_2N_3$ = 518.1616 $[M+Na]^+$, measured 518.1622 $[M+Na]^+$; UV/vis (THF) λ_{max} (ε [M^{-1} cm^{-1}]) 546 (3.1×10^4).

BODIPY 3: Red crystalline solid. Yield: 52 % (73 mg); mp 181 – 182 °C. ^{1}H NMR ($CDCl_3$, 400 MHz, ppm): δ 7.87 (s, 2H), 7.75 (s, 4H), 7.38 (bs, 2H), 6.58 (bs, 2H); ^{13}C NMR ($CDCl_3$, 100 MHz, ppm): 144.8, 136.7, 133.1, 132.5, 129.6, 125.7, 125.6, 119.0, 118.0, 114.2, 101.6, 86.8; ^{11}B NMR ($CDCl_3$, 128 MHz, ppm) 0.14 (t, $J_{B\text{-}F}$ = 29.4 Hz); HRMS (ESI-TOF) m/z = calculated for $C_{18}H10BF_2N_3$ = 340.0831 $[M+Na]^+$, measured 340.0834 $[M+Na]^+$; UV/vis (THF) λ_{max} (ε [M^{-1} cm^{-1}]) 552 (4.4×10^4)

The 2-(4-bromophenyl)-3,3-diphenylacrylonitrile (**e**) was synthesized from previous report.[18]

Synthesis of 2-(4-ethynyltrimethylsilylphenyl)-3,3-diphenylacrylonitrile (d): 1gm (2.78 mol) of 2-(4-bromophenyl)-3,3-diphenylacrylonitrile (**e**) was dissolved in 50ml dry THF and Triethylamine 4:1 mixture. The reaction mixture was degased with argon and trimethylsillyacetylyne (370 µL; 2.33mol), $Pd(PPh_3)_2Cl_2$ (160 mg, 0.14 mol), and CuI (53 mg, 0.27 mol) were added to the reaction mixture. The reaction mixture was refluxed for 24 hours. After complete conversion the reaction mixture was evaporated to dryness and chromatographed on silica gel column chromatography with hexane as eluent. The product was obtained as white colored crystalline solid with 80 % yield. Characterization data: White crystalline solid. Yield: 80 % (840mg); ^{1}H NMR ($CDCl_3$, 400 MHz, ppm): δ 7.46-7.40 (m, 5H), 7.32-7.29 (m, 2H), 7.28-

7.25 (m, 1H), 7.22-7.18 (m, 4H), 7.01-6.98 (m, 2H), 0.24 (s, 9H); ^{13}C NMR ($CDCl_3$, 100 MHz, ppm): 158.5, 140.30, 138.9, 135.0, 132.1, 130.8, 130.1, 130.0, 129.6, 129.3, 128.6, 128.5, 123.1, 119.9, 111.0, 104.5, 96.0, 0.28; HRMS (ESI-TOF) m/z = calculated for $C_{26}H_{23}NSi$ = 400.1492 $[M+Na]^+$, measured 400.1498 $[M+Na]^+$.

Synthesis of 2-(4-ethynyl-phenyl)-3,3-diphenylacrylonitrile (TPAN-alkyne b): The (720mg; 1.9 mol) 2-(4-ethynyltrimethylsilylphenyl)-3,3-diphenylacrylonitrile **d** was dissolved in 60 ml diethylether :methanol (1:3) mixture and was added (393mg; 2.85 mol) K_2CO_3 under argon atmosphere and stirred for 4 hours at room temperature. After complete conversion, the reaction mixture was evaporated to dryness and chromatographed on silica gel column chromatography with dichloromethane: hexane as eluent. The product was obtained as white crystalline solid in 87 % yield. Characterization data: Crystalline solid. Yield: 87 % (506 mg); ^{1}H NMR ($CDCl_3$, 400 MHz, ppm): δ δ 7.47-7.40 (m, 5H), 7.36-7.32 (m, 2H), 7.30-7.26 (m, 1H), 7.24-7.19 (m, 4H), 7.02-6.99 (m, 2H), 3.11 (s, 1H); ^{13}C NMR ($CDCl_3$, 100 MHz, ppm): 158.7, 140.3, 138.9, 135.4, 132.3, 130.8, 130.2, 130.0,129.7, 129.4, 128.6, 128.5, 122.2, 119.9, 110.9, 83.1, 78.7; HRMS (ESI-TOF) m/z = calculated for $C_{23}H_{15}N$ = 328.1097 $[M+Na]^+$, measured 328.1103 $[M+Na]^+$.

Synthesis of 2,3-diphenyl-3-(4-bromophenyl)-acrylonitrile (g): 4-bromobenzophenone (4.46 gm; 0.017 mol), and 60% NaH (0.47gm; 0.020 mol) were dissolved in 20 ml toluene, in three-necked round bottom flask equipped with a condenser under argon atmosphere. The mixture was reflux for 10 min, then benzylnitrile (2gm; 0.017 mol) in 20 ml toluene was added drop wise over 20 min under reflux conditions. During addition reaction mixture turns pink to purple. Evolving H_2 was observed at the oil bubbler. The reaction mixture was stirred for 20 hours. After completion of reaction, the reaction mixture was washed with water and brine. The organic phase was then dried over anhydrous Na_2SO_4 and concentrated under reduced pressure. The yellow oil

was chromatographed on silica gel to obtain desired product as mixture of *cis* and *trans* isomers in 49 % yield. Characterization data: Crystalline solid. Yield: 49 % (3 mg); ^{1}H NMR ($CDCl_3$, 400 MHz, ppm): δ 7.60 (d, *J* = 7.3 Hz, 2H), 7.40-7.35 (m, 5H), 7.33-7.27 (m, 3H), 7.16 (d, *J* = 7.0 Hz, 2H), 7.02 (d, *J* = 7.5 Hz 2H); ^{13}C NMR ($CDCl_3$, 100 MHz, ppm): 157.0, 139.0, 138.2, 133.5, 131.81, 131.78, 131.5, 131.2, 130.6, 129.6, 128.6, 124.6, 122.8, 119.5, 110.8; HRMS (ESI-TOF) m/z = calculated for $C_{21}H_{14}BrN$ = 382.0202 $[M+Na]^+$, measured 382.0213 $[M+Na]^+$.

Synthesis of 2,3-diphenyl-3-(4-ethynyltrimethylsilylphenyl)-acrylonitrile (f): 0.9 gm (2.5 mol) of 2,3-diphenyl-3-(4-bromophenyl)-acrylonitrile (**g**) was dissolved in 50ml dry THF and Triethylamine 4:1 mixture. The reaction mixture was degased with argon and trimethylsillyacetylyne (336 µL; 3 mol), $Pd(PPh_3)_2Cl_2$ (144 mg, 0.125 mol), and CuI (48 mg, 0.25 mol) were added. The reaction mixture was refluxed for 24 hours. After complete conversion the reaction mixture was evaporated to dryness and chromatographed on silica gel column chromatography with hexane as eluent. The product was obtained as mixture of *cis* and *trans* isomers with 74 % yield. Characterization data: White, crystalline solid. Yield: 74 % (700 mg); ^{1}H NMR ($CDCl_3$, 400 MHz, ppm): δ 7.52-7.49 (m, 2H), 7.40-7.38 (m, 2H), 7.28-7.17 (m, 8H), 6.98-6.96 (m, 2H); ^{13}C NMR ($CDCl_3$, 100 MHz, ppm): 156.9, 140.4, 138.8,134.7, 132.1, 130.9, 130.0, 129.8, 129.3, 128.6, 128.4, 124.8, 120.0, 112.0, 104.6, 96.5, 00.0; HRMS (ESI-TOF) m/z = calculated for $C_{26}H_{23}NSi$ = 400.1492 $[M+Na]^+$, measured 400.1491 $[M+Na]^+$.

Synthesis of 2,3-diphenyl-3-(4-ethynylphenyl)-acrylonitrile (c): 2,3-diphenyl-3-(4-ethynyltrimethylsilylphenyl)-acrylonitrile (**f**) (600 mg; 1.59 mol) was dissolved in 60 ml diethylether :methanol (1:3) mixture and was added (2.12 gm; 15.9 mol) K_2CO_3 under argon atmosphere and stirred for 4 hours at room temperature. After complete conversion, the reaction mixture was evaporated to dryness and chromatographed on silica gel column chromatography

with dichloromethane: hexane as eluent. The product was obtained as mixture of *cis* and *trans* isomers in 80 % yield. Characterization data: White, crystalline solid. Yield: 80 % (388 mg); ^{1}H NMR ($CDCl_3$, 400 MHz, ppm): δ 7.64 (d, *J* = 8Hz, 1H), 7.53 (m, 2H), 7.41-7.29 (m, 8H), 7.08 (t, *J* = 8Hz, 2H), 3.36-3.21 (2×s, 1H); ^{13}C NMR ($CDCl_3$, 100 MHz, ppm): 156.79, 156.75, 140.8, 140.0, 139.6, 138.8, 134.65, 134.61, 132.3, 132.0, 130.9, 130.85, 130.2, 130.0, 129.8, 129.3, 128.76, 128.73, 128.68,128.63, 128.5, 123.81, 122.86, 119.97, 119.94, 112.4, 112.2, 83.2, 83.1, 79.1, 78.9; HRMS (ESI-TOF) m/z = calculated for $C_{23}H_{15}N$ = 328.1097 $[M+Na]^+$, measured 328.1112 $[M+Na]^+$.

Acknowledgement

We thank DST, New Delhi for financial support. BD and TJ thank CSIR and UGC New Delhi for their fellowships. We are thankful to Sophisticated Instrumentation Centre (SIC), IIT Indore.

Supporting Information

Text, figures, tables, and CIF files giving general experimental methods, ^{1}H, ^{13}C, ^{11}B, and ^{19}F NMR and HRMS spectra of all new compounds, crystallographic data for **2a** and **2b** (CCDC numbers 1401617 and 1401616 respectively), DFT calculation data and electrochemical studies. This material is available free of charge via the Internet at http://pubs.acs.org.

1 (a) Lu, H.; Mack, J.; Yang, Y.; Shen, Z. *Chem. Soc. Rev.* **2014**, *43*, 4778; (b) Loudet, A.; Burgess, K. *Chem. Rev.* **2007**, *107*, 4891; (c) Han, J.; Burgess, K. *Chem. Rev.* **2010**, *110*, 2709.

2 (a) Yin, X.; Li, Y.; Li, Y.; Zhu, Y.; Tang, X.; Zheng, H.; Zhu, D. *Tetrahedron* **2009**, *65*, 8373; (b) Yin, X.; Li, Y.; Zhu, Y.; Jing, X.; Li, Y.; Zhu, D. *Dalton Trans.* **2010**, *39*, 9929; (c) Awuah, S. G.; You, Y. *RSC Adv.* **2012**, *2*, 11169; (d) Boens, N.; Leen, V.; Dehaen, W. *Chem. Soc. Rev.*

2012, *41*, 1130; (e) Kim, H. S.; Pham, T. C. T.; Yoon, K. B. *Chem. Commun.* **2012**, *48*, 4659; (f) Benniston, A. C.; Copley, G. *Phys. Chem. Chem. Phys.* **2009**, *11*, 4124.

3 (a) Nepomnyashchii, A. B.; Bard, A. J. *Acc. Chem. Res*. **2012**, *45*, 1844; (b) Boens, N.; Leen, V.; Dehaen, W. *Chem. Soc. Rev*. **2012**, *41*, 1130; (c) Tamgho, I.-S.; Hasheminasab, A.; Engle, J. T.; Nemykin, V. N.; Ziegler, C. J. *J. Am. Chem. Soc.* **2014**, *136*, 5623; (d) Yokoi, H.; Wachi, N.; Hiroto, S.; Shinokubo, H. *Chem. Commun.* **2014**, *50*, 2715; (e) Bessette, A.; Hanan, G. S. *Chem. Soc. Rev.* **2014**, *43*, 3342; (f) Dhokale, B.; Gautam, P.; Mobin, S. M.; Misra, R. *Dalton Trans.*, **2013**, *42*, 1512; (g) Misra, R.; Dhokale, B.; Jadhav, T.; Mobin, S. M. *Organometallics*, 2014, **33**, 1867–1877; (h) Dhokale, B.; Jadhav, T.; Mobin, S. M.; Misra, R. *Dalton Trans.*, **2015**, DOI: 10.1039/C5DT00565E.

4 (a) Ulrich, G.; Ziessel, R.; Harriman, A. *Angew. Chem. Int. Ed.* **2008**, *47*, 1184; (b) Yakubovskyi, V. P.; Shandura, M. P.; Kovtun, Y. P. *Eur. J. Org. Chem.* **2009**, *2009*, 3237; (c) Shandura, M. P.; Yakubovskyi, V. P.; Kovtun, Y. P. *Org. Biomol. Chem.* **2013**, *11*, 835.

5 Dhokale, B.; Jadhav, T.; Mobin, S. M.; Misra, R. *Chem. Commun.* **2014**, *50*, 9119.

6 (a) Kusaka, S.; Sakamoto, R.; Kitagawa, Y.; Okumura, M.; Nishihara, H. *Chem. – Asian J.* **2013**, *8*, 723; (b) Graf, K.; Korzdorfer, T.; Kummel, S.; Thelakkat, M. *New J. Chem.* **2013**, *37*, 1417; (c) Misra, R.; Dhokale, B.; Jadhav, T.; Mobin, S. M. *Dalton Trans.* **2013**, *42*, 13658.

7 (a) Misra, R.; Dhokale, B.; Jadhav, T.; Mobin, S. M. *Dalton Trans.* **2014**, *43*, 4854; (b) Misra, R.; Dhokale, B.; Jadhav, T.; Mobin, S. M. *New J. Chem.* **2014**, *38*, 3579; (c) Misra, R.; Jadhav, T.; Dhokale, B.; Gautam, P.; Sharma, R.; Maragani, R.; Mobin, S. M. *Dalton Trans.* **2014**, *43*, 13076; (d) Flores-Rizo, J. O., Esnal, I., Osorio-Martínez, C. A., Gómez-Durán, C. F. A., Bañuelos, J., López Arbeloa, I., Pannell, K. H.; Metta-Magaña, A. J.; Peña-Cabrera, E. *J. Org. Chem.*, **2013**, *78*, 5867.

8 Hong, Y,; Lam, J. W. Y.; Tang, B. Z. *Chem. Soc. Rev*., **2011**, *40*, 5361.

9 (a) Dong, Y.; Lam, J. W. Y.; Qin, A.; Liu, J.; Li, Z.; Tang, B. Z.; Sun, J.; Kwok, H. S. *Appl. Phys. Lett.* **2007**, *91*, 011111; (b) Huang, J.; Yang, X.; Wang, J.; Zhong, C.; Wang, L.; Qin, J.; Li, Z. *J. Mat. Chem.* **2012**, *22*, 2478; (c) Zhao, N.; Yang, Z.; Lam, J. W. Y.; Sung, H. H. Y.; Xie, N.; Chen, S.; Su, H.; Gao, M.; Williams, I. D.; Wong, K. S.; Tang, B. Z. *Chem. Commun.* **2012**, *48*, 8637; (d) Misra, R.; Jadhav, T.; Dhokale, B.; Mobin, S. M. *Chem. Commun*. **2014**, *50*, 9076; (e) Jadhav, T.; Dhokale, B.; Mobin, S. M.; Misra, R. *RSC Adv*. **2015**, *5*, 29878.

10 (a) An, B.-K.; Kwon, S.-K.; Jung, S.-D.; Park, S. Y. *J. Am. Chem. Soc.* **2002**, *124*, 14410; (b) Gong, Y.; Tan, Y.; Liu, J.; Lu, P.; Feng, C.; Yuan, W. Z.; Lu, Y.; Sun, J. Z.; He, G.; Zhang, Y. *Chem. Commun.* **2013**, *49*, 4009.

11 Leen, V.; Yuan, P.; Wang, L.; Boens, N.; Dehaen, W. *Org. Lett.* **2012**, *14*, 6150.

12 Zhao, Z.; Chen, S.; Lam, J. W. Y.; Jim, C. K. W.; Chan, C. Y. K.; Wang, Z.; Lu, P.; Deng, C.; Kwok, H. S.; Ma, Y.; Tang, B. Z. *J. Phys. Chem. C* **2010**, *114*, 7963.

13 (a) Wang, S.; Oldham, W. J.; Hudack, R. A.; Bazan, G. C. *J. Am. Chem. Soc.* **2000**, *122*, 5695; (b) Yuan, W. Z.; Gong, Y.; Chen, S.; Shen, X. Y.; Lam, J. W. Y.; Lu, P.; Lu, Y.; Wang, Z.; Hu, R.; Xie, N.; Kwok, H. S.; Zhang, Y.; Sun, J. Z.; Tang, B. Z. *Chem. Mat.* **2012**, *24*, 1518.

14 Petrushenko, I. K.; Petrushenko, K. B. *Spectrochim. Acta Mol. Biomol. Spectrosc.* **2015**, *138*, 623.

15 Li, Y.; Liu, T.; Liu, H.; Tian, M. Z.; Li, Y. *Acc. Chem. Res.* **2014**, 47, 1186.

16 Boens, N.; Wang, L.; Leen, V.; Yuan, P.; Verbelen, B.; Dehaen, W.; Van der Auweraer, M.; De Borggraeve, W. D.; Van Meervelt, L.; Jacobs, J.; Beljonne, D.; Tonnelé, C.; Lazzaroni, R.; Ruedas-Rama, M. J.; Orte, A.; Crovetto, L.; Talavera, E. M.; Alvarez-Pez, J. M. *J. Phys. Chem. A* **2014**, *118*, 1576.

17 Gabe, Y.; Urano, Y.; Kikuchi, K.; Kojima, H.; Nagano, T. *J. Am. Chem. Soc.* **2004**, *126*, 3357.

18 Sunahara, H.; Urano, Y.; Kojima, H.; Nagano, T. *J. Am. Chem. Soc.* **2007**, *129*, 5597.

19 (a) Baglan, M.; Ozturk, S.; Gur, B.; Meral, K.; Bozkaya, U.; Bozdemir, O. A.; Atlgan, S. *RSC Adv.* **2013**, *3*, 15866; (b) Li, Z.; Chen, Y.; Lv, X.; Fu, W.-F. *New J. Chem.* **2013**, *37*, 3755; (c) Li, Z.; Zheng, M.; Guan, X.; Xie, Z.; Huang, Y.; Jing, X. *Nanoscale* **2014**, *6*, 5662; (d) Zhang, S.; Wang, Y.; Meng, F.; Dai, C.; Cheng, Y.; Zhu, C. *Chem. Commun.* **2015**, *51*, 9014; (e) Hu, R.; Gomez-Duran, C. F. A.; Lam, J. W. Y.; Belmonte-Vazquez, J. L.; Deng, C.; Chen, S.; Ye, R.; Pena-Cabrera, E.; Zhong, Y.; Wong, K. S.; Tang, B. Z. *Chem. Commun.* **2012**, *48*, 10099.

20 Gritzner, G.; Kuta, G. J. *Pure Appl. Chem.* **1984**, *56*, 461.